Molecular Dynamics in Shape Space and Femtosecond Vibrational Spectroscopy of Metal Clusters

Constantine Yannouleas and Uzi Landman*

School of Physics, Georgia Institute of Technology, Atlanta, Georgia 30332-0430

Received: December 4, 1997; In Final Form: February 5, 1998

We introduce a method of molecular dynamics in shape space aimed at metal clusters. The ionic degrees of freedom are described via a dynamically deformable jellium with inertia parameters derived from an incompressible, irrotational flow. The shell correction method is used to calculate the electronic potential energy surface underlying the dynamics. Our finite-temperature simulations of Ag_{14} and its ions, following the negative-to-neutral-to-positive scheme, demonstrate the potential of pump-and-probe ultrashort laser pulses as a spectroscopy of cluster shape vibrations.

The study of the motion of an incompressible and irrotational fluid mass with an ellipsoidal surface has its origins in investigations on the theory of the shape of the Earth. Such studies started with Newton and Maclaurin and were continued by others, in particular for the case of a *varying* surface by Dirichlet, Dedekind, and Riemann (see ref 1). In these early studies in the realm of astronomy and astrophysics, the forces were due to the gravitational field. More recently, similar ideas were used in nuclear physics in investigations of low-energy collective isoscalar modes[2] (as well as of the fission process[3] in atomic nuclei). Additionally, many features of the analysis of these nuclear collective modes[2] go back to the work of Rayleigh on the normal modes of a classical liquid drop.[4]

In this Letter, we introduce and apply a method of molecular dynamics in shape space (MDSS) aimed at studies of materials clusters, with the potential energy surfaces (PES's), which underlie the dynamics, determined via electronic structure calculations using the shell correction method (SCM),[5−8] and with inertia parameters specified according to the aforementioned theory of an irrotational fluid mass.

In the past several years, first-principles molecular-dynamics (FPMD) simulation methods, where the dynamics of the ions is evaluated on concurrently calculated electronic PES's [e.g., through local density functional (LDF) theory], have been introduced and employed in investigations of atomic and molecular clusters.[9,10] The MDSS method complements such techniques. Rather than simulating the dynamical trajectories of the individual ions as in other FPMD methods, the MDSS focuses on the dynamics of *collective shape variations* of clusters[11] (with the ionic degrees of freedom described via a dynamically deformable jellium), allowing for reliable and economical simulations in a broad cluster size range.

Over the past several years, the development and application of fast spectroscopical techniques opened new avenues for probing dynamical processes in matter (both in the molecular and condensed-phase regimes) with unprecedented temporal resolution (in the femtosecond range[12]). As an illustration, we apply the MDSS to an investigation of the shape dynamics of a small neutral cluster (Ag_{14}), motivated by recent experiments using pump-and-probe ultrashort laser pulses. In these experiments, referred to as NeNePo,[13] negative-to-neutral-to-positive, mass-selected neutral clusters are prepared by electron vertical detachment from the associated negative ions, and their subsequent time evolution is probed by photoionization, which can be time-delayed with reference to the initial detachment. Our finite-temperature MDSS simulations of Ag_{14} and of associated ions, following the NeNePo sequence, demonstrate the potential of such experiments as a spectroscopy of cluster shape vibrations. As the jellium description of metal clusters is known to be most adequate above the Debye temperature, Θ_D, we demonstrate the MDSS method for cluster shape dynamics at $T > \Theta_D(\mathrm{Ag})$ (=215 K).

Modeling the dynamics of the ellipsoidal jellium background as that of an irrotational, incompressible fluid, its kinetic energy is given[1] by

$$\mathcal{T}(a, b) = (2/15)\pi\rho a' b' c'(\dot{a}'^2 + \dot{b}'^2 + \dot{c}'^2) \qquad (1)$$

where ρ is the mass density of the fluid and a', b', and c' are the principal semiaxes of the ellipsoid. Since the PES $V(a', b')$ depends only on two semiaxes, we can eliminate the third semiaxis c' from the kinetic energy by using the volume conservation, namely, $a'b'c' = R^3$. By further defining reduced semiaxes $a = a'/R$, $b = b'/R$, and $c = c'/R$, we can rewrite the kinetic energy as

$$\mathcal{T}(a, b) = {}^1/_2 M_{aa}\dot{a}^2 + M_{ab}\dot{a}\dot{b} + {}^1/_2 M_{bb}\dot{b}^2 \qquad (2)$$

where the elements of the inertial-mass matrix M are $M_{aa} = C(1 + 1/a^4b^2)$, $M_{ab} = M_{ba} = C/a^3b^3$, and $M_{bb} = C(1 + 1/a^2b^4)$, with $C = 4\pi R^5\rho/15$.

At constant energy, the motion of the shape will be governed by Hamilton's equations associated with the Hamiltonian $H = \mathcal{T}(a, b) + V(a, b)$. Introducing new symbols $a \leftrightarrow q_1$, $b \leftrightarrow q_2$, $p_a \leftrightarrow p_1$, and $p_b \leftrightarrow p_2$, for the generalized coordinates a and b and for the associated canonical momenta p_a and p_b, Hamilton's equations of motion are given by

$$\dot{q}_i = \sum_{j=1}^{2} (M^{-1})_{ij} p_j \qquad (3)$$

$$\dot{p}_i = \frac{\partial V}{\partial q_i} - \frac{1}{2}\sum_{j,k=1}^{2} \frac{\partial (M^{-1})_{jk}}{\partial q_i} p_j p_k \qquad (4)$$

S1089-5639(98)00407-1 CCC: $15.00
Published on Web 03/20/1998

where M^{-1} is the inverse of the inertial-mass matrix M. These equations are solved using a sixth-order Runge−Kutta method.

MDSS simulations can be carried out at constant energy or constant temperature. The latter (canonical-ensemble) simulations can be achieved through a straightforward modification of Hamilton's equations according to the Nosé−Hoover-thermostat prescription,[14] namely, by adding a variable friction term $-p_i\eta/Q$ to the right-hand side of the $\dot{p}_i$ equation, where Q is a constant characterizing the reservoir and $\eta = 2\mathcal{T}(q_1, q_2) - 2k_BT$, with T the temperature and k_B the Boltzmann constant. Since, however, the triaxial MDSS involves two independent variables only, we use a chain[15] of three Nosé−Hoover thermostats in order to guarantee that the equilibrium ensemble will exhibit canonically distributed positions and momenta.

The SCM approach has been derived by us originally from the LDF theory (for details, see refs 5 and 7). This method, as well as a semiempirical version[6,7] of it which we employ here to determine the PES's [i.e., V in eq 4], has been shown to yield accurate results[5−7,8,16] when compared to experiments and/or self-consistent Kohn−Sham LDF calculations (when available) for several metal-cluster systems. Particularly pertinent to this study are SCM results for the vertical ionization potential (vIP) of Ag_{14} and the electron vertical detachment energy (vDE) of Ag_{14}^-; the SCM results, calculated for the equilibrium configurations, are vIP = 5.84 eV and vDE = 2.20 eV, in excellent agreement with measured values, vIP = 5.90 eV[17] and vDE ∼ 2.2 eV.[18]

We prepare first an equilibrium ensemble of 10^3 phase-space points [$(q_1)_0$, $(q_2)_0$, $(p_1)_0$, and $(p_2)_0$] of the anion (Ag_{14}^-) by selecting them from a long trajectory (up to 400 ps) on the PES of Ag_{14}^- generated using the Nosé−Hoover dynamics at a given temperature T. These phase-space points are subsequently used as initial values for generating shorter (up to 3 ps), constant-energy trajectories,[19] with an integration time step of 0.5 fs,[20] on the PES of the neutral Ag_{14} (which is produced from the anion by electron photodetachment caused by the first laser pulse). At each time step, we determine the classical probability, P(t), that vertical ionization of the dynamically evolving neutral cluster is energetically allowed through the two-photon absorption process induced by the probe-laser pulse. P(t) is that fraction of the instantaneous shape configurations (averaged over the 10^3 constant-energy trajectories) with a vertical ionization potential vIP ≤ $2\hbar\omega$, where $\hbar\omega$ is the single-photon energy.

The probability P(t) is a classical quantity that in principle is not the sole factor determining the yield of the photoionization process (e.g., the photoion current of the cationic daughters). Indeed the photoion current is proportional to the product of the classical P(t) with the quantum mechanical, vibrational, Franck−Condon overlap factor.[21] If the neutral clusters happen to be produced in shape configurations far away from the PES minima of the positive ion, the Franck−Condon overlap factor can be so low initially that virtually no positive ions are generated, regardless of the value of P(t), and thus the onset of the photoion current can exhibit a characteristic delay. The NeNePo experiment for the silver trimer conforms to this case.[13,22] However, the case of Ag_{14} is different, since here the PES minima of the neutral and the positive clusters overlap substantially (see Figure 1). As a result, in the latter case, the Franck−Condon factor for the ionization process is close to unity, and we can safely assume that the photoion current is mainly proportional to the classical probability P(t).

In Figure 1, we display the PES's for Ag_{14}^- (bottom panel), Ag_{14} (middle), and Ag_{14}^+ (top). For the neutral Ag_{14}, which is axially symmetric, there are two energetically distinct isomers−

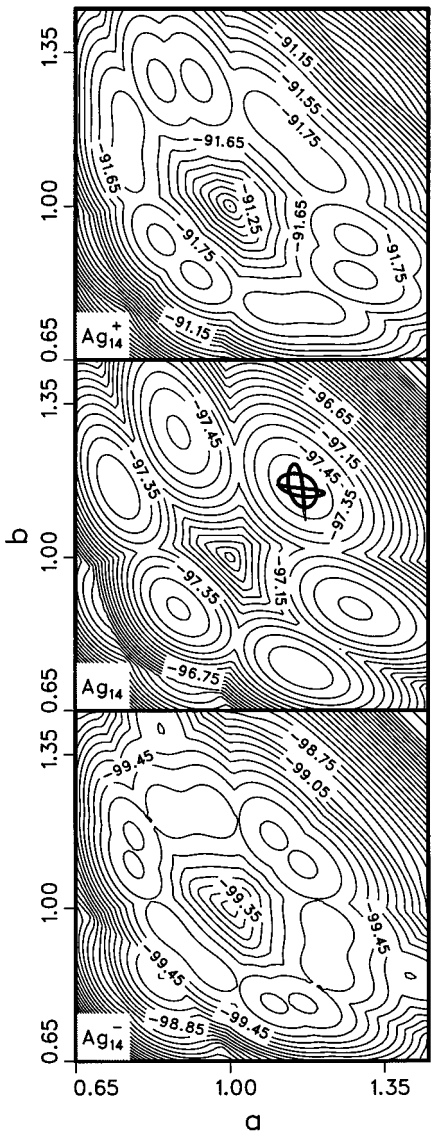

Figure 1. PES's of Ag_{14}^- (bottom panel), Ag_{14} (middle), and Ag_{14}^+ (top). a and b denote dimensionless semiaxes of the ellipsoidal shapes (the third semi-axis $c = 1/ab$; see text for details). The contour lines correspond to increments of 0.1 eV in the total energy of the clusters. The Lissajous-type figure (heavy solid line), inside one of the basins associated with the oblate isomer of Ag_{14}, portrays one of the 3-ps, constant-energy trajectories at T = 300 K (see text).

an oblate (O) one and a prolate (P) one. On the associated PES (Figure 1, middle panel), there are six local minima, three (energetically degenerate ones) corresponding to the oblate O-isomer (having two equal axes larger than unity; the case $a = b > 1$ with $c = 1/a^2$ is easily identifiable; the other two follow by circular permutation of the indices a, b, and c, i.e., pseudorotations) and the other three (energetically degenerate ones) to the P-isomer (having two equal axes smaller than unity; the case of $a = b < 1$ with $c = 1/a^2$ is also easily identifiable, and the other two are obtained via pseudorotations). The positive and negative ions are slightly triaxial, and as a result their PES's exhibit 12 local minima, six of them close to oblate shapes and the other six close to prolate shapes; in each case, the six minima are energetically degenerate and are related to each other via pseudorotations.

At T = 300 K, the canonical-ensemble distribution of the initial 10^3 phase-space points on the PES of Ag_{14}^- is distributed about the O-like minima, since for the anion these minima are

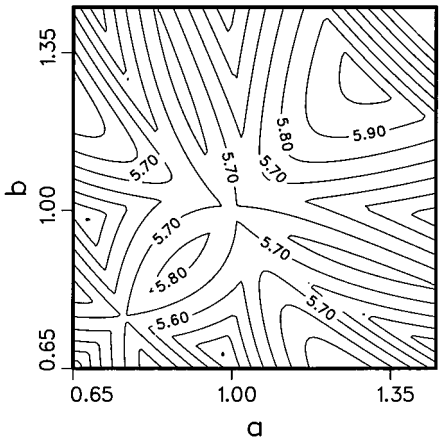

Figure 2. vIP surface for Ag_{14}. The contour lines correspond to increments of 0.1 eV. *a* and *b* denote dimensionless semiaxes of the ellipsoidal shapes (the third semiaxis $c = 1/ab$).

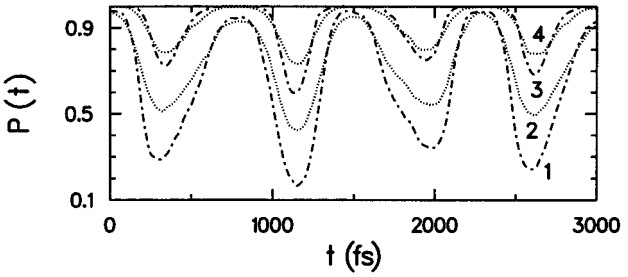

Figure 3. Time evolution of the probability P(*t*) (see text) for $T = 300$ K (dashed−dotted lines) and $T = 600$ K (dotted lines). The two-photon energy of the photoionizing probe-laser pulse equals 5.85 eV (lower pair of curves labeled 1 and 2) and 5.90 eV (upper pair of curves labeled 3 and 4).

the global ones by ≈0.06 eV (or 700 K) compared to the P-like minima. As a result of the vertical photodetachment, some of the initial shapes will land on the basins of the P-minimum of the neutral Ag_{14}; nevertheless most of the initial shapes will land on the basins of the O-minimum. For the neutral Ag_{14}, these latter basins are deep, separated from the basins of the P-minimum by a barrier of ≈0.35 eV (i.e., 4060 K), and thus only initial O-shapes associated with momenta far in the tails of the canonical distribution will be able to make excursions outside these basins. Consequently, the majority of the (constant-energy) trajectories of Ag_{14} will correspond to shape vibrations around the O-minimum (see the Lissajous-type trajectory in the middle panel of Figure 1).

To investigate how these vibrations can be probed by a photoionizing laser pulse of a given frequency, we display in Figure 2 the vIP surface [which is the difference between the PES of the cation and that of the neutral Ag_{14} (see Figure 1)]. It is noteworthy that the local minima of the neutral Ag_{14} do not correspond to extrema in the vIP's. Indeed the O-minimum has a vIP of 5.85 eV, which is intermediate between the extremal values of 6.0 and 5.7 eV. Consequently, a photoionizing laser pulse with photon energy $2\hbar\omega = 5.85$ eV is ideal for probing the vibrations about the O-minimum, since the ionization condition vIP $\leq 2\hbar\omega$ will be satisfied only for certain segments of the constant-energy trajectories, and thus the measured photoionization yield will exhibit oscillations reflecting the shape vibrations.

An inspection of the probability P(*t*) (which is displayed in Figure 3) corroborates indeed the above analysis and in addition allows for determination of the period of the shape vibrations around the O-minimum of Ag_{14}. For $T = 300$ K (lower dashed−dotted curve labeled 1), the probability P(*t*) exhibits large-amplitude oscillations with a period of ≈800 fs. Raising the temperature of the initial Ag_{14}^- ensemble tends to progressively smear out the oscillatory structure in P(*t*). This behavior is a consequence of the fact that the distribution of the initial phase-space points on the PES of the anion is more spread away from the region of the O-like minima (a relatively larger amount of initial points is distributed over the region of the P-like minima). As a result, a larger, but still not dominant, fraction of constant-energy trajectories on the PES of Ag_{14} is restricted to the regions inside the basins of the P-minima. For $T = 600$ K (lower dotted curve labeled 2), the effect of such trajectories is to reduce the amplitude of the oscillations of the P(*t*) curve. We also note here that for the range of temperatures considered (which covers the experimentally expected range) no influence on the period of the oscillations is predicted.

With a somewhat larger probe-laser frequency (e.g., $2\hbar\omega = 5.90$ eV), the ionization condition vIP $\leq 2\hbar\omega$ is satisfied for longer segments of the constant-energy trajectories, and as a result the troughs in the P(*t*) curve are now less accentuated compared to the case of $2\hbar\omega = 5.85$ eV (see upper curves labeled 3 and 4 in Figure 3).

We remark that the experiments suggested in our paper, and the NeNePo experiments performed in ref 13, involve electron detachment and ionization of clusters, and they can be performed with photon energies that are away from the plasmon excitations of silver clusters, which otherwise would have complicated the interpretation of such experiments owing to resonant photoabsorption.[23]

In summary, a molecular dynamics in shape space method for simulating the dynamics of low-frequency collective modes associated with metal-cluster shapes was introduced. These collective modes (adiabatic in the Born−Oppenheimer sense) are analogous to the well-known low-energy isoscalar vibrations of atomic nuclei.[2] The ionic degrees of freedom were described via a dynamically deformable jellium with inertia parameters derived from an incompressible, irrotational flow, and the shell correction method was used to calculate the electronic potential energy surface underlying the dynamics of the cluster shape. Our finite-temperature simulations of Ag_{14} and its ions, following the negative-to-neutral-to-positive scheme, serve to illustrate the MDSS method and demonstrate the potential of pump-and-probe ultrashort laser pulses as a spectroscopy of cluster shape vibrations.

We further remark that the MDSS method can be generalized to provide a dynamical theory for metal-cluster fission (see refs 9a, 24−26). In analogy with recent dynamical nuclear fission studies,[27] such a theory will provide efficient means for calculating fission rates, branching ratios between fission channels, and the dynamics of fission isomers (refs 9a, 25), as well as the kinetic energy distribution[25] of the fission fragments for a broad range of cluster sizes.

Acknowledgment. This research is supported by the U.S. Department of Energy (Grant No. FG05-86ER-45234). Studies were performed at the Georgia Institute of Technology Center for Computational Materials Science.

References and Notes

(1) Lamb, H. *Hydrodynamics*; Cambridge University Press: New York, 1945; p 719.

(2) Bohr Å.; Mottelson, B. R. *Nuclear Structure*; Benjamin: Reading, MA, 1975; Vol. II.

(3) Owing to the generalized shapes associated with the fission process, Werner and Wheeler developed a special numerical method for calculating the inertia parameters of an incompressible, irrotational nuclear flow with axial symmetry (see: Davies, K. T. R.; Sierk, A. J.; Nix, J. R. *Phys. Rev. C* **1976**, *13*, 2385).

(4) Rayleigh, J. W. S. *Theory of Sound*; MacMillan: London, 1877.

(5) Yannouleas, C.; Landman, U. *Phys. Rev. B* **1993**, *48*, 8376; *Chem. Phys. Lett.* **1993**, *210*, 437.

(6) Yannouleas, C.; Landman, U. *Phys. Rev. B* **1995**, *51*, 1902.

(7) Yannouleas, C.; Landman, U. In *Large Clusters of Atoms and Molecules*; Martin, T. P., Ed.; Kluwer: Dordrecht, 1996; p 131.

(8) Yannouleas, C.; Landman, U. *Phys. Rev. Lett.* **1997**, *78*, 1424.

(9) (a) Barnett, R. N.; Landman, U.; Rajagopal, G. *Phys. Rev. Lett.* **1991**, *67*, 3058. (b) Barnett, R. N.; Landman, U. *Phys, Rev. B* **1993**, *48*, 2081.

(10) Röthlisberger, U.; Andreoni, W. *J. Chem. Phys.* **1991**, *94*, 8129.

(11) In the case of FPMD methods, such collective shape oscillations may be analyzed by considering the time variations of the moments of inertia of the clusters and/or the eccentricity parameter, which can be calculated from the positions of the individual ions. For certain small sodium clusters this was done in ref 10, where it was found that the shape oscillations occur on a time scale of 350−500 fs, comparable to the results obtained by us in the present study of Ag_{14}.

(12) *Ultrafast Phenomena IX*; Barbara, P. F., Knox, W. H., Mourou, G. A., Zewail, A. H., Eds; Springer Series in Chemical Physics 60; Springer: Berlin, 1994. Zewail, A. H. *J. Phys. Chem.* **1996**, *100*, 12701.

(13) Wolf, S.; Sommerer, G.; Rutz, S.; Schreiber, E.; Leisner, T.; Wöste, L. *Phys. Rev. Lett.* **1995**, *74*, 4177.

(14) Nosé, S. *J. Chem. Phys.* **1984**, *81*, 511. Hoover, W. G. *Phys. Rev. A* **1985**, *31*, 1695.

(15) Martyna, G. J.; Klein, M. L.; Tuckerman, M. *J. Chem. Phys.* **1992**, *97*, 2635.

(16) In this paper, we use the semiempirical version of the SCM approach. In the case of Ag_N clusters, the parameters entering into these calculations are $U_0 = -0.045$, $r_s = 3.01$ au, $t = 0.47$ au, $\delta_0 = 0$ for the cations, $\delta_0 = 1.31$ au for the anions, $\delta_2 = 0$, $W = 4.26$ eV, $\alpha_v = -8.061$ eV, $\alpha_s = 2.05$ eV, and $\alpha_c = 0.86$ eV (see ref 6 for the meaning of these parameters). The mass of the delocalized valence electrons was taken equal to the free-electron mass. For the coinage metals (e.g., Cu, Ag, and Au), contributions from atomic d electrons enter mainly through the value of the work function (W), and to a lesser extent through the surface tension (α_s) and curvature (α_c) coefficients, which are chosen to coincide with the experimental values, rather than with those derived through jellium-LDA calculations (for details, see ref 6).

(17) Alameddin, G.; Hunter, J.; Cameron, D.; Kappes, M. M. *Chem. Phys. Lett.* **1992**, *192*, 122.

(18) Taylor, K. J.; Pettiette-Hall, C. L.; Cheshnovsky, O.; Smalley, R. E. *J. Chem. Phys.* **1992**, *96*, 3319.

(19) To simulate energy exchange between the dynamical collective shape variables and the other degrees of freedom of the cluster, one can include frictional terms in the equations of motion. This would result in damping of the collective shape dynamics; for the short trajectories used here, such effects are not expected to have a significant influence.

(20) In our constant-energy simulations, the total energy is conserved within 10^{-7} eV. In the case of the Nosé−Hoover dynamics, the associated pseudo-energy is conserved within 10^{-6} eV.

(21) Herzberg, G. *Spectra of Diatomic Molecules*; D. Van Nostrand Co.: New York, 1950; p 194.

(22) Our model provides a natural framework for calculating the Franck−Condon overlap factors $\int \psi_{v'} \psi_v \, da db$ (see ref 21) by allowing within the shape space for the calculation of the vibrational wave functions $\psi_v(a, b)$, which depend on the generalized, semiaxes coordinates a and b. In analogy with studies on transition nuclei, we propose to specify $\psi_v(a, b)$ by solving the nonlinear Bohr−Mottelson Hamiltonian (see: Kumar, K.; Baranger, M. *Nucl. Phys. A* **1967**, *92*, 608). Work along this line for the NeNePo of the silver trimer is in progress.

(23) The experiments in ref 13 used photons of 3.1 eV for electron detachment and (double) photons of 5.9−6.36 eV for ionization, while the plasmon energy in small silver clusters is about 4.0 eV and decreases almost linearly to about 3.5 eV (which is the bulk Mie value) for larger ones (see: Liebsch, A. *Electronic Excitations at Metal Surfaces*; Plenum: New York, 1997; Figure 3.56; p 138). Similarly in our study, the required electron-detachment energy is about 2.2 eV and the ionization potentials are also away from the plasmon energy (i.e., 5.7−6.0 eV, see Figure 2).

(24) Yannouleas, C.; Landman, U. *J. Phys. Chem.* **1995**, *99*, 14577. Yannouleas, C.; Barnett, R. N.; Landman, U. *Comments At. Mol. Phys.* **1995**, *31*, 445.

(25) Bréchignac, C.; Cahuzac, P.; Carlier, F.; de Frutos, M.; Barnett, R. N.; Landman, U. *Phys. Rev. Lett.* **1994**, *72*, 1636.

(26) When using jellium clusters in conjunction with a volume-conserving two-center model[24] in the context of fission processes, the energetically favored fission products correspond to integer numbers of atoms (see Figure 2 in: Mustafa, M. G.; Mosel, U.; Schmitt, H. W. *Phys. Rev. C* **1973**, *7*, 1519 and ref 24).

(27) Carjan, N.; Wada, T.; Abe, Y. In *AIP Conf. Proc.* **1991**, *250*, 230.